LOCKHEED MARTIN ENERGY RESEARCH LIBRARIES

3 4456 0514955 9

ORNL-TM-3959

cy. 28

NEUTRON SENSOR DEVELOPMENT FOR EXTREME ENVIRONMENTS PROGRESS REPORT FOR PERIOD JANUARY 1, 1971, TO JUNE 30, 1972

LIBRARY
REFERENCE COPY

OAK RIDGE NATIONAL LABORATORY
OPERATED BY UNION CARBIDE CORPORATION • FOR THE U.S. ATOMIC ENERGY COMMISSION

Printed in the United States of America. Available from
National Technical Information Service
U.S. Department of Commerce
5285 Port Royal Road, Springfield, Virginia 22151
Price: Printed Copy $3.00; Microfiche $0.95

This report was prepared as an account of work sponsored by the United States Government. Neither the United States nor the United States Atomic Energy Commission, nor any of their employees, nor any of their contractors, subcontractors, or their employees, makes any warranty, express or implied, or assumes any legal liability or responsibility for the accuracy, completeness or usefulness of any information, apparatus, product or process disclosed, or represents that its use would not infringe privately owned rights.

ORNL-TM-3959
UC-79m – Liquid Metal Fast
Breeder Reactors
(Instrumentation and Controls)

Contract No. W-7405-eng-26

INSTRUMENTATION AND CONTROLS DIVISION

NEUTRON SENSOR DEVELOPMENT FOR EXTREME ENVIRONMENTS

Progress Report for Period
January 1, 1971, to June 30, 1972

D. P. Roux

with contributions from

A. R. Buhl
F. J. Davis
G. C. Guerrant
W. T. Clay
J. T. De Lorenzo
D. W. Gidley*
J. C. Robinson**

DECEMBER 1972

*Albion College, Albion, Michigan.

**Consultant from the Dept. of Nuclear Engineering, the University of Tennessee, Knoxville.

OAK RIDGE NATIONAL LABORATORY
Oak Ridge, Tennessee 37830
Operated by
UNION CARBIDE CORPORATION
for the
U. S. ATOMIC ENERGY COMMISSION

LOCKHEED MARTIN ENERGY RESEARCH LIBRARIES

3 4456 0514955 9

ABSTRACT

Basic investigations in fission counter development were made for application in the hostile in-core environment of LMFBR's. The studies comprised analyses, digital computations, and experiments to optimize the gamma rejection of fission counters and to formulate the gamma pile-up effect, shielding effect on the gamma response, and selection of gamma shields for fission counters. Electron drift velocity data were evaluated, and new data were obtained. From these studies, general considerations for optimization of fission counters were summarized. The electrical shield performance of high-temperature, mineral-insulated coaxial cables was tested, and electronic noise in current pulse preamplifiers was reduced. The design characteristics of a fission counter for operation at 750°F were determined. A detector was designed with a sensitivity of 1 count/sec-nv at a gamma flux of 3×10^6 R/hr.

CONTENTS

		Page
1.	Introduction	1
2.	Detector Optimization Studies	1
	2.1 Formulation of the GPU Effect in Fission Counters	3
	2.2 Effect of Shielding on the Gamma Response of a Neutron Detector	10
	2.3 Selection of a Gamma Shield for Fission Counters	17
	2.4 Electron Drift Velocity	19
3.	Electronics Development	30
	3.1 Electrical Shield Performance of High-Temperature MI Coaxial Cables	32
	3.2 Reduction of Electronic Noise in Current-Pulse Preamplifier	32
4.	Design and Test of High Temperature Fission Counter	32
	4.1 Design Characteristics of a 750°F Fission Counter	34
	4.2 Mechanical Characteristics	34
	4.3 Sensitivity Data	35

1. INTRODUCTION

A program was continued to develop neutron sensors that will have unusually high gamma-rejection capability for operation during reactor startup and to enable subcriticality measurement of the reactor at extremely high temperature and in the hostile in-core environment of a Liquid-Metal Fast Breeder Reactor (LMFBR). Table 1 illustrates the detector environment and requirements for such applications. The ultimate objective of this program is to develop a fission counter with a sensitivity of 1 count/sec-nv and which will be qualified for operation at 1100°F in a gamma background of 10^6 R/hr.

To achieve this objective, the scope of the program includes three basic areas: (1) detector optimization studies, (2) electronics development, and (3) design and tests of high-temperature fission counters and MI cable. For such demanding gamma rejection performances, the factors that affect detector optimization must be thoroughly analyzed and understood. In addition, the pulse electronics for signal processing must be designed such that the entire detection system, as well, is optimum. The detector-preamplifier must be operated in the current mode (Fig. 1) to achieve the best gamma rejection performance.

2. DETECTOR OPTIMIZATION STUDIES

Analytical studies, digital computations, and experiments were performed to optimize the gamma rejection of fission counters. The first study was to formulate the gamma pile-up (GPU) effect on fission counters so that the sensitivity of GPU to gamma flux ϕ_γ and detector parameters such as the electron collection time τ could be evaluated.

Experimental work consisted of testing various detectors in a gamma facility to evaluate the detector sensitivity to the gamma-ray energy and to assess the need and effectiveness of a gamma shield surrounding the detector. Detailed computation was performed to support these experiments and to evaluate the perturbing effect of shielding material on the detector neutron sensitivity in order to select an adequate shield.

Table 1. Detector environment and requirements

MINIMUM 10 COUNTS/SEC FOR STARTUP

↓

LOCATION IN REACTOR VESSEL (REFLECTOR OR SHIELD)

↓

ENVIRONMENT DURING STARTUP:

- GAMMA FIELD 10^6-10^7 R/hr
- OPERATING TEMPERATURE 800-1000°F
- SURVIVAL TEMPERATURE 1200°F
- MECHANICAL VIBRATIONS CAUSED BY PARTIAL SODIUM FLOW

↓

DETECTOR REQUIREMENTS:

>10 COUNTS/SEC FROM NEUTRONS: NEUTRON SENSITIVITY ~1 COUNT/(sec - $n\bar{v}_{th}$)

<1 COUNT/SEC FROM BACKGROUND (GAMMA, ELECTRICAL NOISE, ETC.)

RUGGEDNESS AND RELIABILITY

Drift velocities of gas and gas-mixture candidates for use in fission counters were compiled from the literature and experimentally determined at ORNL when unavailable.

2.1 Formulation of the GPU Effect in Fission Counters

An expression was derived and experimentally verified that expresses the amplitude distribution of the GPU as a function of the gamma flux ϕ_γ and detector parameters such as the electron collection time τ. These data will enable fission counter users and designers to accurately predict the GPU effect in their detector applications.

For a pulse detector operated in the current mode[1] (Fig. 1), individual pulses can be approximated as rectangular current pulses of amplitude q/τ and duration τ (Fig. 2), q being the electrical charge collected as a result of a detection. For a fission counter, the charge q_n produced by a fission (neutron interaction) is $\sim 10^3$ greater than that produced by a gamma interaction q_γ. Accordingly, a single neutron pulse can, in principle, be separated from a single gamma pulse by pulse height discrimination. However, in large gamma fluxes, the gamma pulse rate $\phi_\gamma r_\gamma$ (where r_γ is the pulse rate per flux unit) is so high that gamma pulses cannot be detected individually. For example, at 10^6 R/hr, $\phi_\gamma r_\gamma$ would be about 3×10^{11} pulses/sec, and, if the electron collection time were 10^{-7} sec, an average of 3×10^4 gamma interactions would occur (pile-up) per unit time τ. In such a gamma field, the output current from the counter would be continuous, with a mean component and a fluctuating component due to the statistical nature of the detection process. The mean component of the gamma-induced signal could be blocked with a high-pass filter, but the amplitude of the fluctuating component could be large enough to pass through the pulse height discriminator and, hence, contribute to the observed counts.

To determine the dependence of the observed gamma counts on the gamma pulse rate $\phi_\gamma r_\gamma$ and the properties of the detector, we first considered the mean number of gamma pulses in time 2τ, which is $2\phi_\gamma r_\gamma \tau$. Because the events are randomly distributed, they obey Poisson's distribution; the standard deviation of the number of

ORNL-DWG 72-6756R

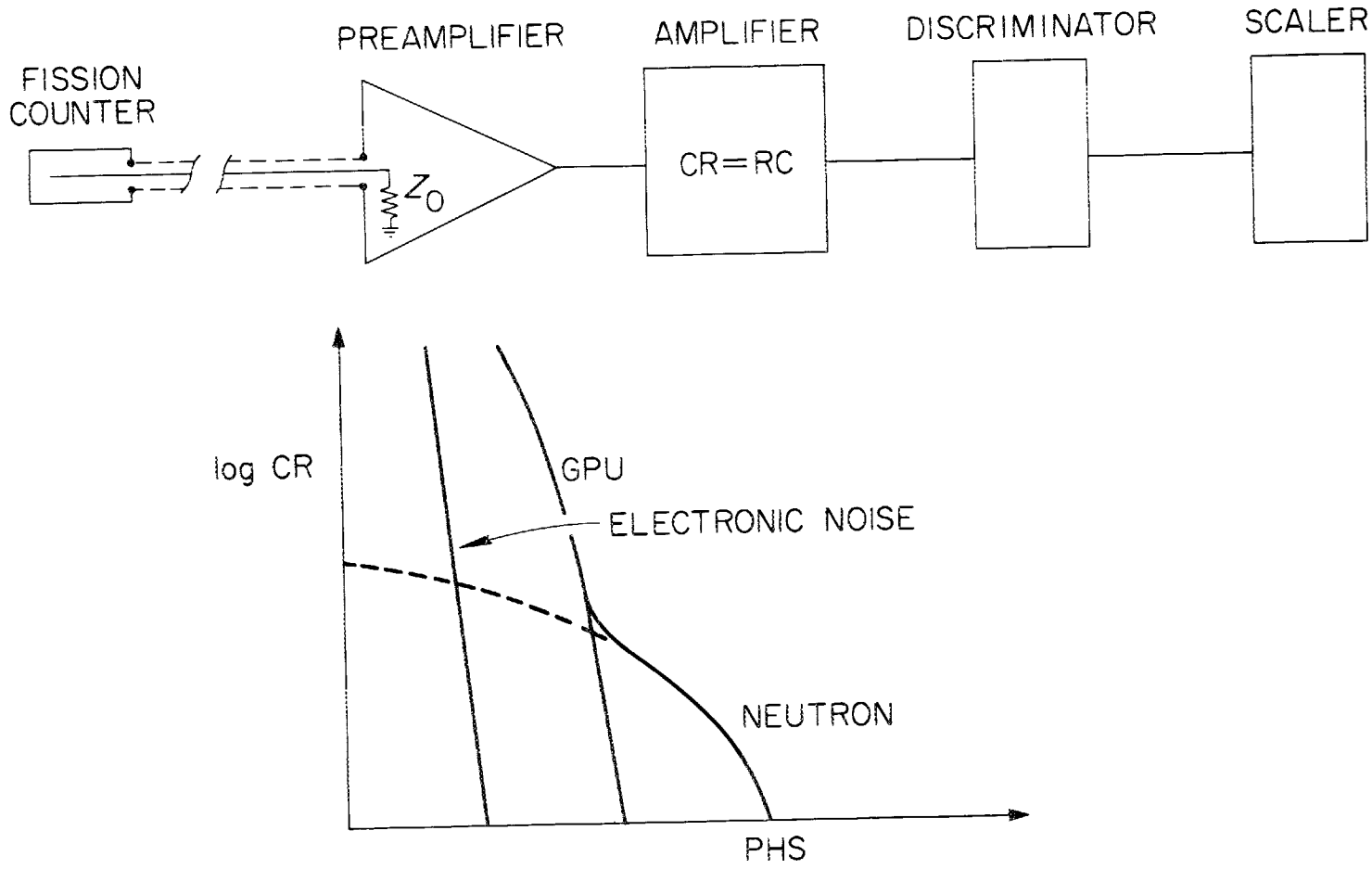

Fig. 1. Diagram of a fission counter detection system operating in the current mode.

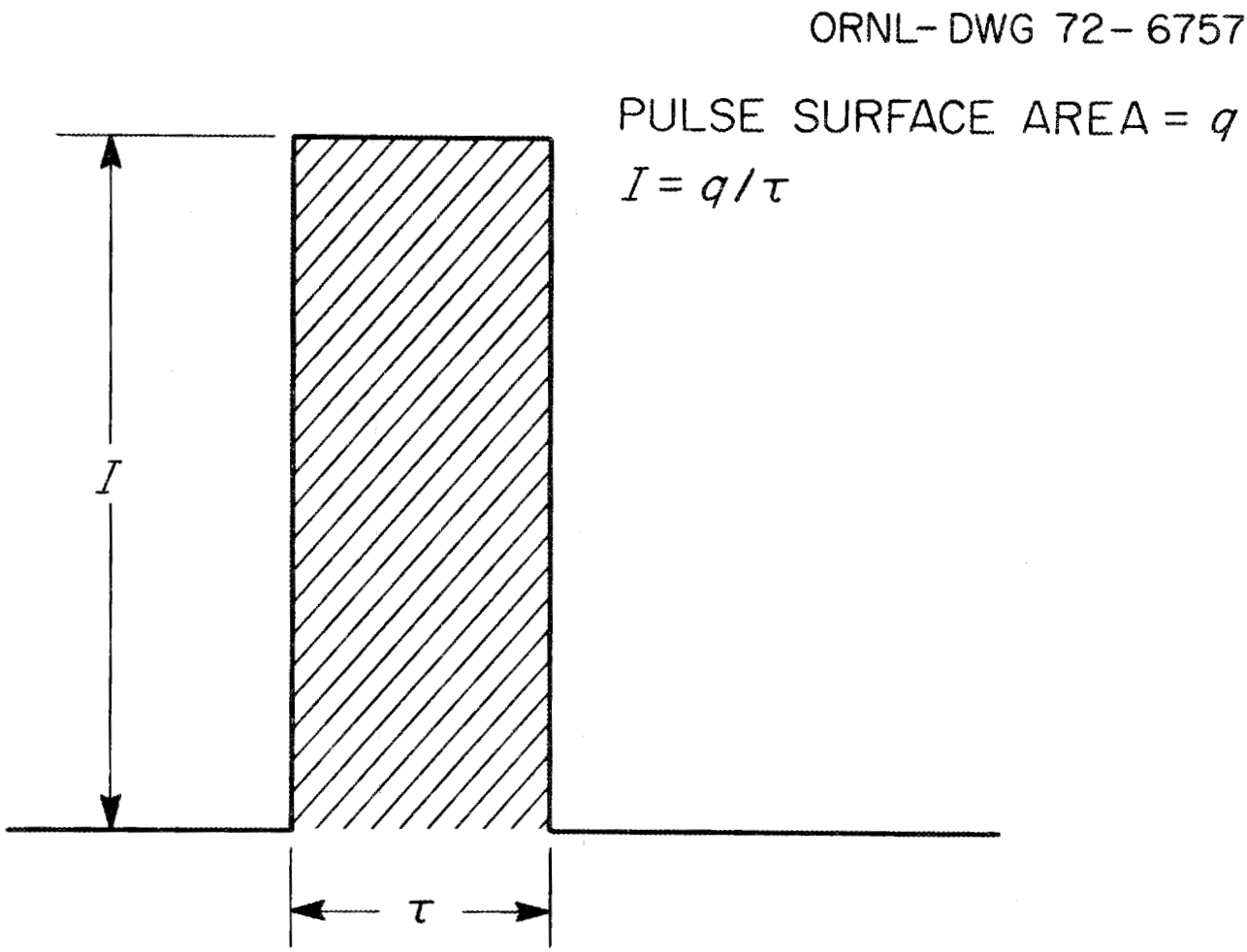

Fig. 2. Idealized pulse shape for a fission counter operated in current-mode amplification.

events is $(2\phi_\gamma r_\gamma \tau)^{1/2}$. Each gamma pulse has a mean height of $\bar{q}_\gamma/\tau$; accordingly, the standard deviation of the amplitude of the gamma-induced current $\sigma_\gamma(i)$ is

$$\sigma_\gamma(i) = \frac{\bar{q}_\gamma}{\tau}(2\phi_\gamma r_\gamma \tau)^{1/2} = \left(\frac{2\phi_\gamma r_\gamma}{\tau}\right)^{1/2} \bar{q}_\gamma . \qquad (1)$$

Using the properties of the normal distribution function, we constructed a GPU function vs discriminator setting in standard deviation units (Fig. 3). Then we verified the shape and amplitude of this analytic GPU distribution with experimentally observed GPU distributions.

Analysis of Eq. (1) implies that the GPU distribution function is proportional to $\phi_\gamma^{1/2}$ and $\tau^{-1/2}$ (instead of being proportional to ϕ_γ and independent of τ, as accepted prior to this study). This dependence of the GPU distribution on $\phi_\gamma^{1/2}$ and $\tau^{-1/2}$ was verified experimentally (Fig. 4), using the neutron detection system described in ref. 2. In particular, when the gamma field was increased a factor of 5, the observed average net amplitude of the GPU distribution* increased a factor of 2.24, which compares favorably with the predicted factor of $\sqrt{5} = 2.24$.

The $\tau^{-1/2}$ dependence of the GPU (Fig. 5) was evaluated by varying the gas filling composition of the same fission counter (95% Ar - 5% CO_2 vs 99% Ar - 1% N_2, yielding measured collection times τ of 85 and 105 nsec, respectively). When the average amplitude of the GPU distribution was measured at 10^7 R/hr with both gas fillings, the average amplitude was 1.11 times greater for the fission counter filled with the "faster" gas. This ratio of 1.11 is precisely equal to $(85/105)^{-1/2}$.

We demonstrated that the GPU effect can be understood and predicted by considering the statistical nature of the detection process. In particular, the analytical

---

*The observed amplitude of the GPU distribution includes the electronic noise amplitude distribution. To obtain the net amplitude of the GPU distribution, the electronic noise contribution must be subtracted:

$$PHS_{net} = (PHS^2_{obs} - PHS^2_{noise})^{1/2} .$$

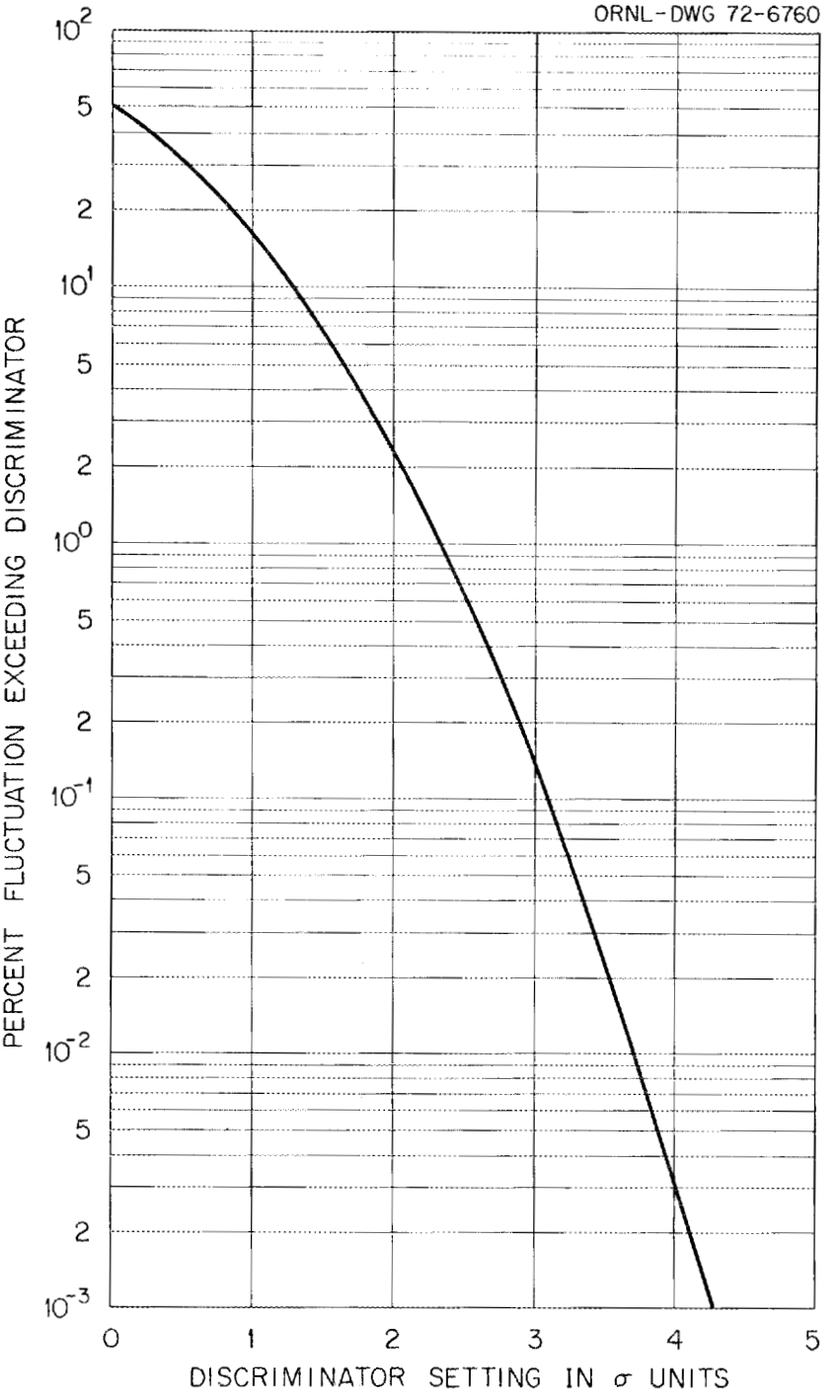

Fig. 3. Calculated gamma pile-up (GPU) function vs discriminator setting in standard deviation units.

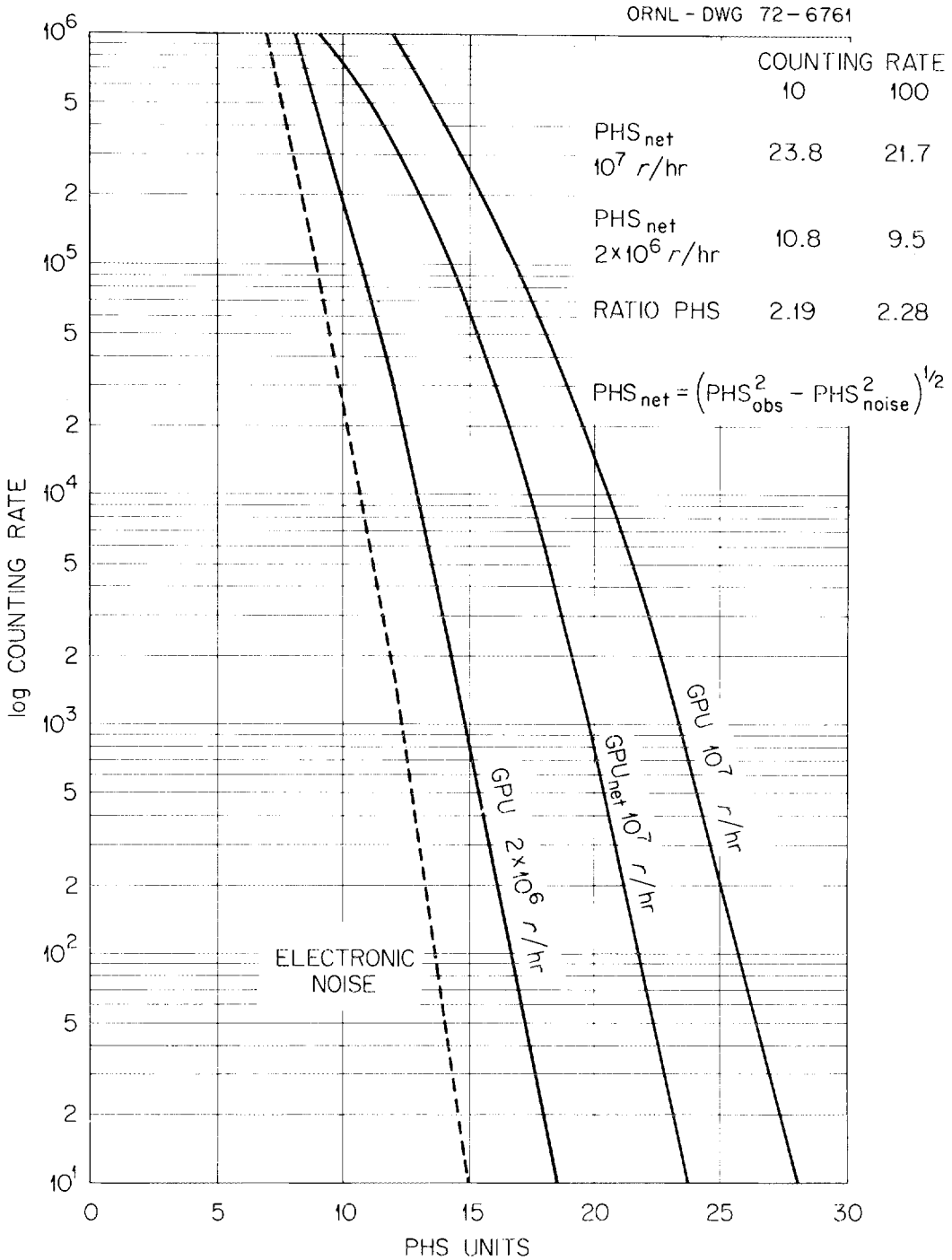

Fig. 4. Dependence of GPU distribution on $\phi_\gamma^{1/2}$ (τ = constant).

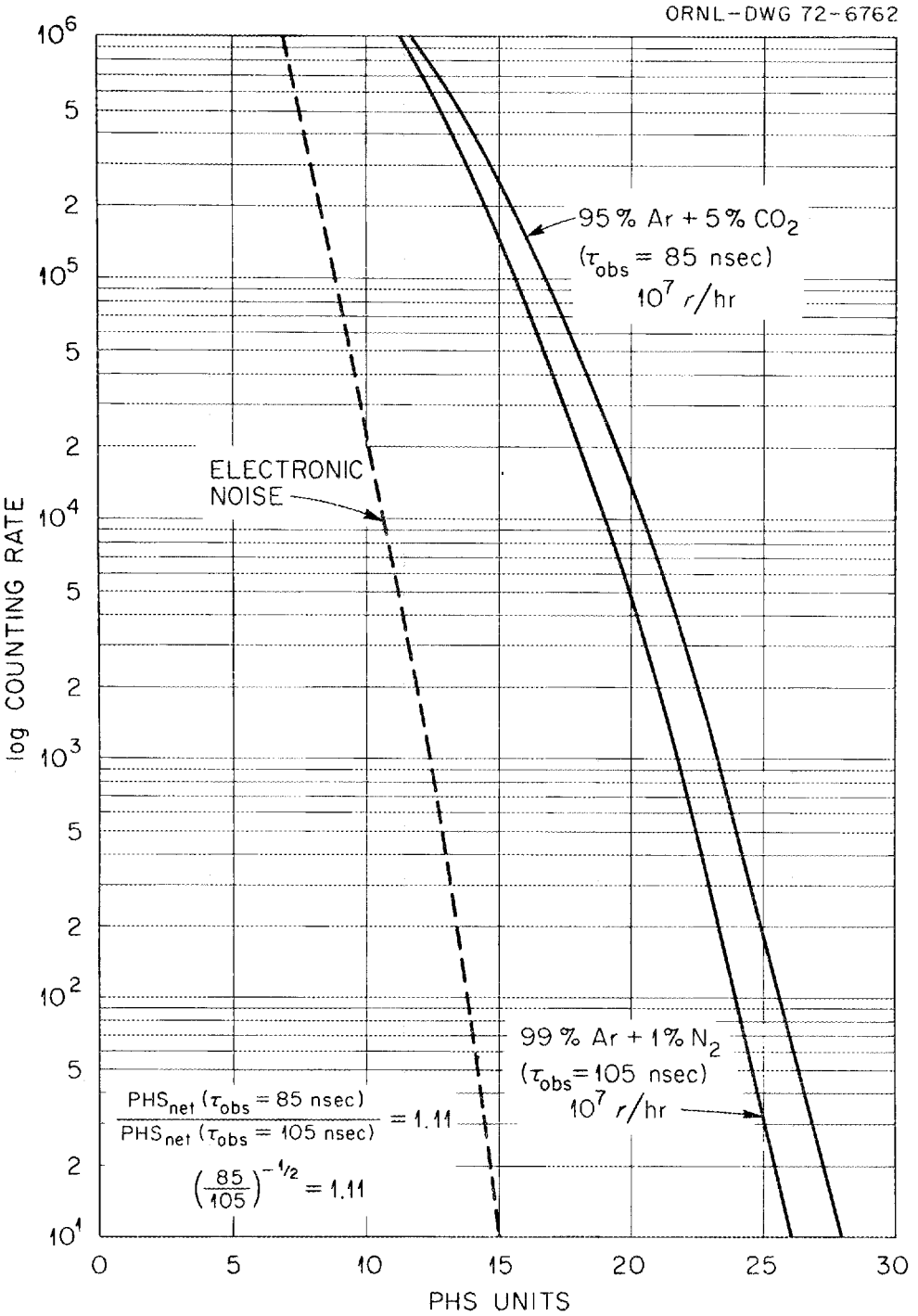

Fig. 5. Dependence of GPU distribution on $\tau^{-1/2}$ ($\phi_\gamma = 1.0 \times 10^7$ R/hr).

and experimental GPU distribution vs pulse height setting agree well, and the GPU distribution function is proportional to $\phi_\gamma^{1/2}$ and $\tau^{-1/2}$.

2.2 Effect of Shielding on the Gamma Response of a Neutron Detector

Experimental studies were made with three neutron detectors in a gamma facility to evaluate their GPU sensitivity to gamma energy. The detectors were

1. An ORNL PCP II-102 fission counter with Ti electrodes[2] and filled with 99% AR - 1% N_2 to 2 atm.
2. An ORNL PCP II-100 ionization chamber that is almost identical to the PCP II-102, but does not have ^{235}U-coated electrodes and does have a 31% greater electrode surface area.
3. An RSN-81A ionization chamber with Al electrodes and filled with 5 atm of ^3He. This detector structure is identical to an RSN-76A.

The detectors were tested for GPU sensitivity with a 25,000-Ci ^{60}Co source. The apparatus consisted of a tank in which a source and detectors could be positioned to allow a desired separation distance. Lead shields of various thicknesses could be installed around the detectors. The response of the detectors to 1.25-MeV gamma rays from the ^{60}Co was first determined with the tank empty. Then the tank was filled with water, and the response of the detectors to low-energy gamma rays was determined (the water degrades the energy of the ^{60}Co photons).

Three experimental conditions were used: (a) detectors and source in air, with a source centerline to detector centerline separation of 12 in., (b) detectors and source in water, separated 15 in., and (c) detectors and source in water, separated 6 in. For these three configurations, Pb shields of 0.135 in. and 0.375 in. were used.

Equation (1) can also be formulated as

$$\sigma_\gamma(i) = [2\phi_\gamma r_\gamma \bar{q}_\gamma (\bar{q}_\gamma/\tau)]^{1/2}$$

$$= [2\phi_\gamma S_\gamma (\bar{q}_\gamma/\tau)]^{1/2}$$

$$= [2\, I_{DC_\gamma} (\bar{q}_\gamma/\tau)]^{1/2}$$

Gamma pile-up is proportional to $I_{DC_\gamma}^{1/2}$, and, for these GPU experimental studies, the measured detector response was simply the detector I_{DC} output.

With the detectors and source in air, the results (Fig. 6) show that attenuation by Pb is well approximated by the narrow-beam attenuation assumption.

With the detectors and source in water (Figs. 7 and 8), attenuation by Pb is well approximated by narrow-beam attenuation considerations, at least for Pb shield thicknesses more than 0.1 in. For shield thicknesses less than 0.1 in., there is a significant "hook" in the I_{DC} attenuation curve. These hooks are caused by low-energy gamma rays, and a small amount of shielding will absorb such low-energy radiation.

The low-energy effects are more pronounced as the detector-source separation becomes greater because the ^{60}Co gamma-ray energy spectrum is degraded by the water to a greater degree as the detector-source separation is increased (Figs. 9 and 10). These figures show gamma-ray-energy spectra calculated using the one-dimensional transport code ANISN[3] for the two separation distances of 15 and 6 in., respectively, with no Pb. The spectra are for an RSN-81A aluminum electrode configuration, calculated for the center of the sensitive volume (spectra for several points inside and near the outside of the detector were also calculated and were nearly identical for a given detector-source separation distance).

A second conclusion from these experimental results is that the low-energy effects are greater with PCP II-110 detectors (Ti electrodes and filled with Ar) than for the RSN-81A detector (Al electrodes and filled with ^3He). At gamma energies below 0.3 MeV, the total mass absorption coefficient μ varies greatly as a function of the structural materials and gases, and, as a result, gas and wall effects vary significantly. Above 0.3 MeV, wall effects are generally invariant, and the detector sensitivity S_γ per cubic centimeter of sensitive volume at 0°C and 760 mm pressure for a gas different from air is closely

$$S_\gamma = 0.927 \times 10^{-13} \frac{A - hr}{r - cm^3} \times \left(\frac{Z_{gas}}{Z_{air}} \times \frac{W_{air}}{W_{gas}} \right),$$

where Z is the atomic number, and W is the energy per ion pair.

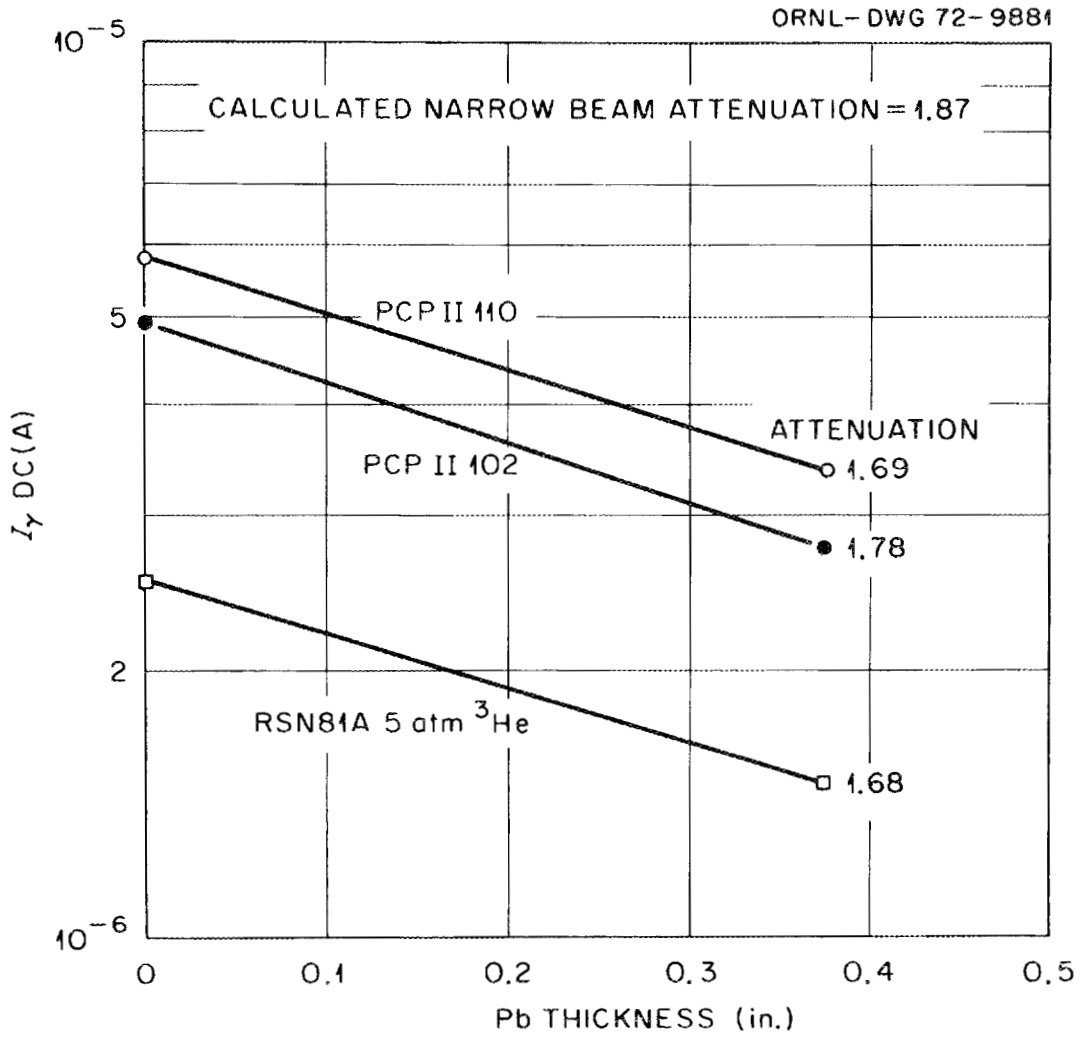

Fig. 6. I_{DC_γ} as a function of Pb thickness for detector and source in air, with a separation distance of 12 in.

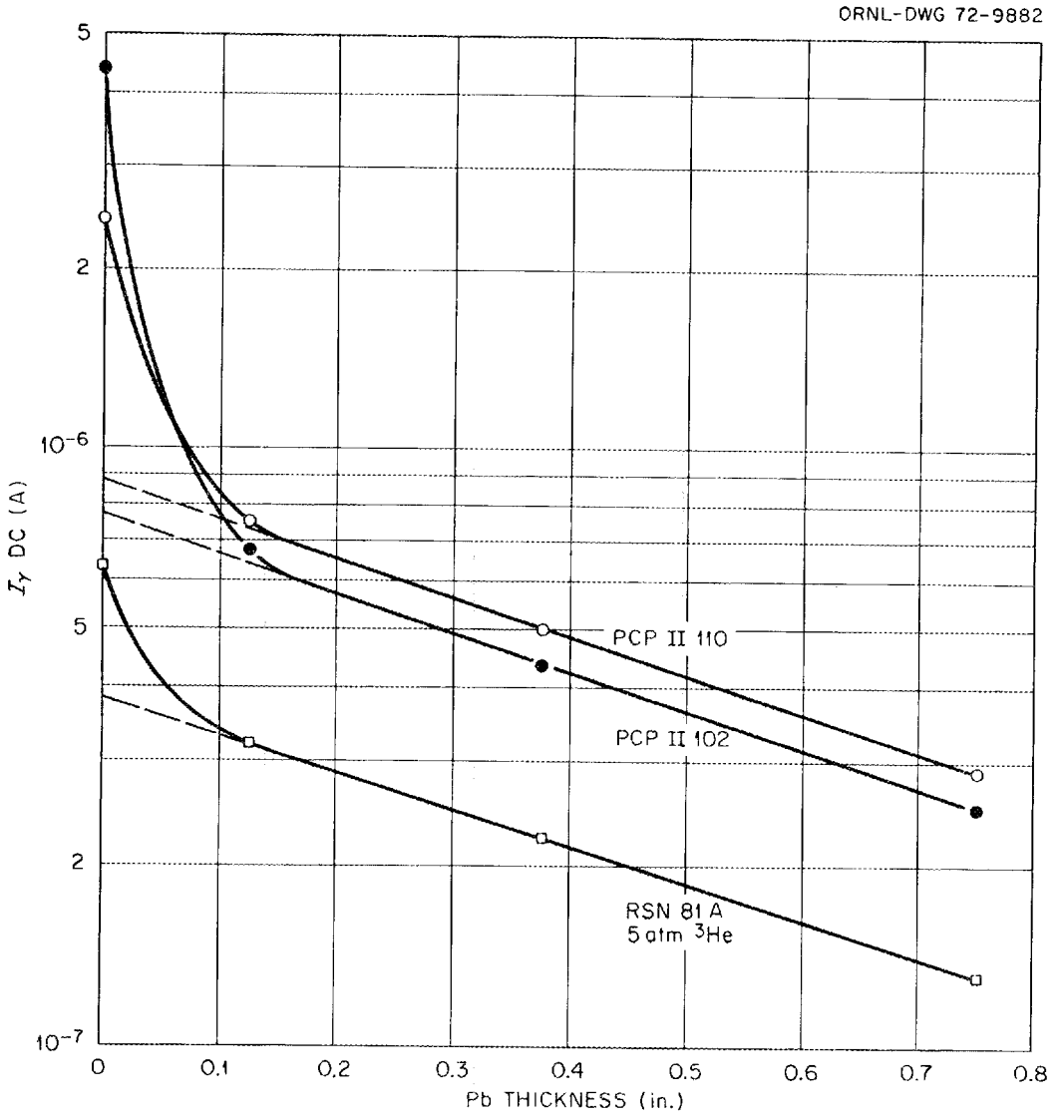

Fig. 7. I_{DC_γ} as a function of Pb thickness for detector and source in water, with a separation distance of 15 in.

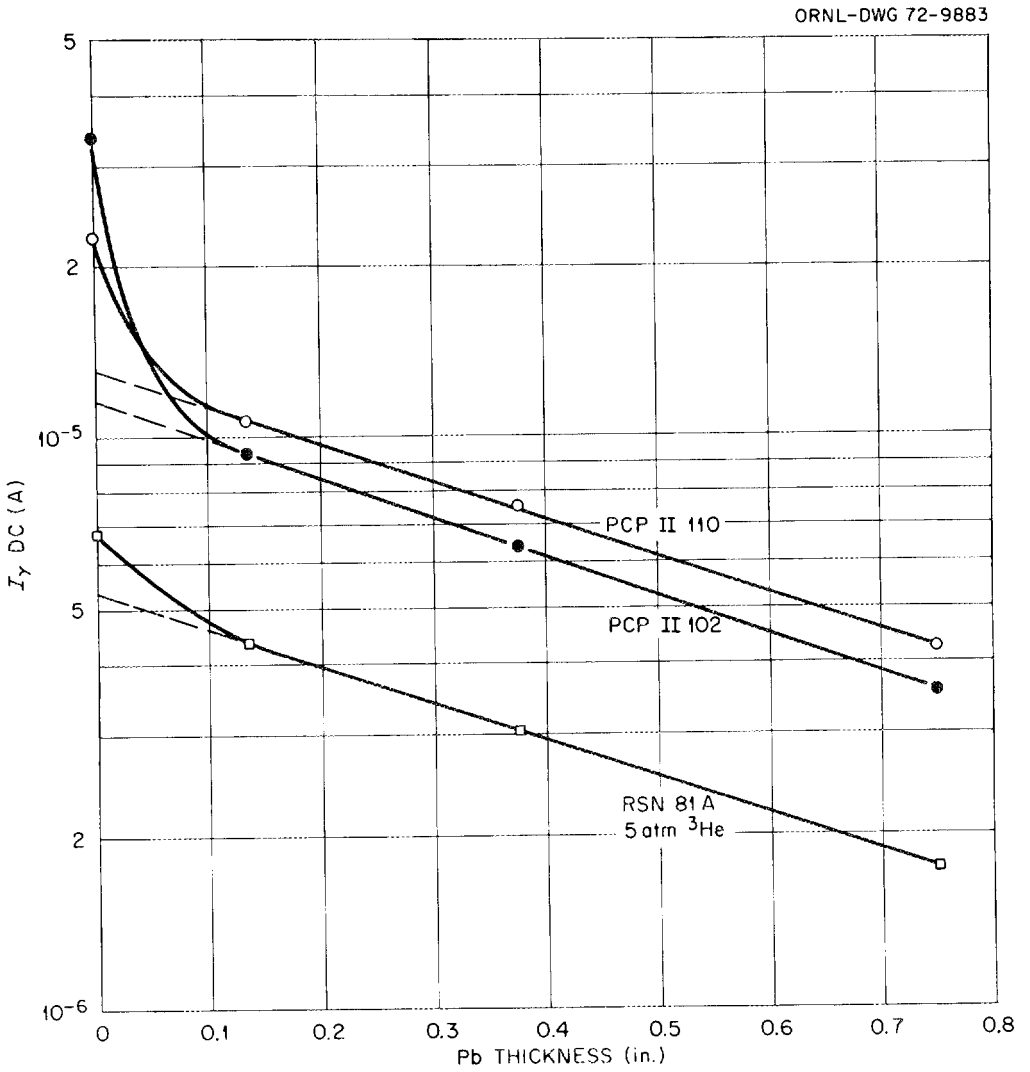

Fig. 8. I_{DC_γ} as a function of Pb thickness for detector and source in water, with a separation distance of 6 in.

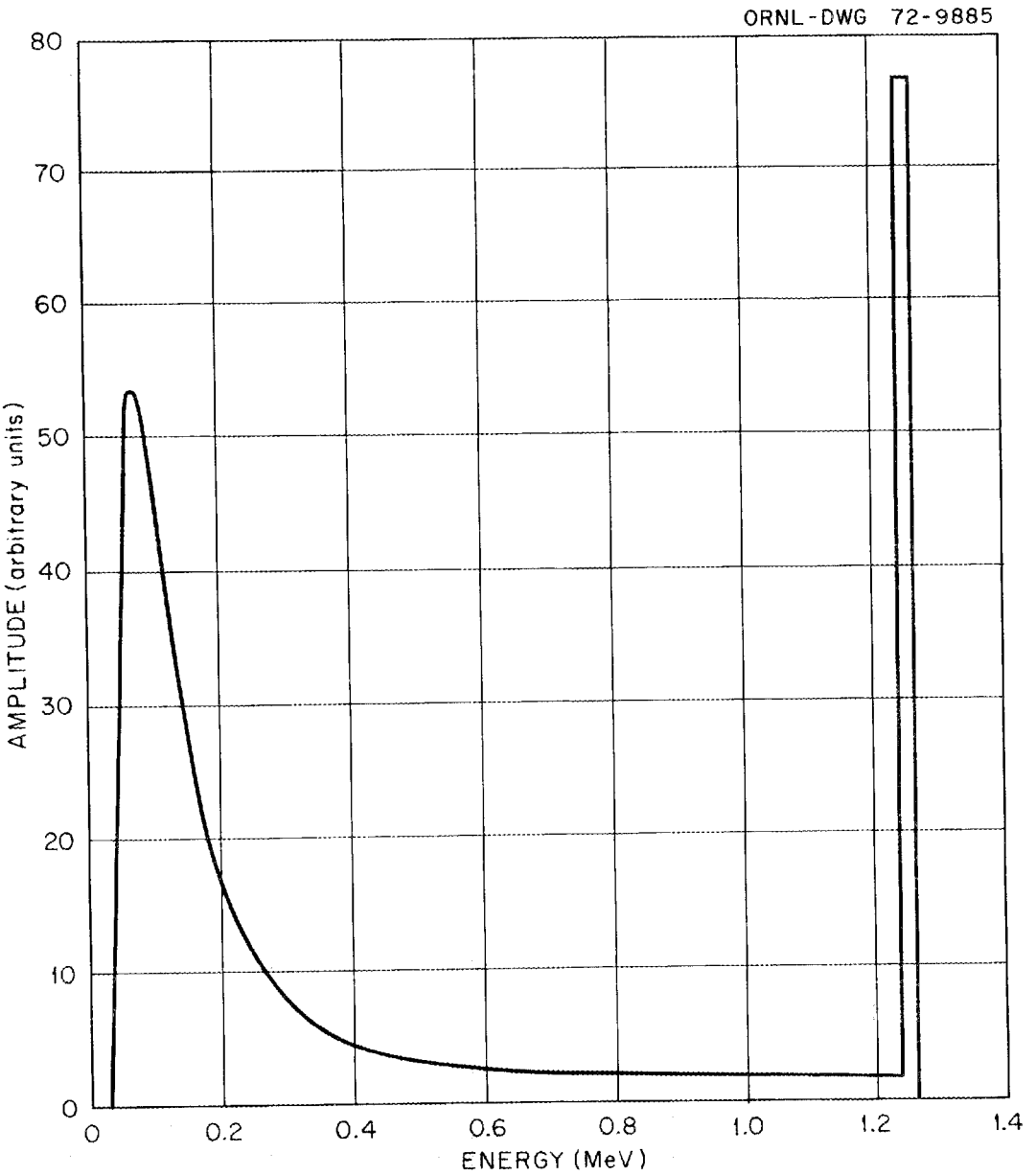

Fig. 9. Calculated gamma-ray energy spectrum at the center of an RSN-81A detector, with water between the detector and ^{60}Co source and a separation distance of 15 in.

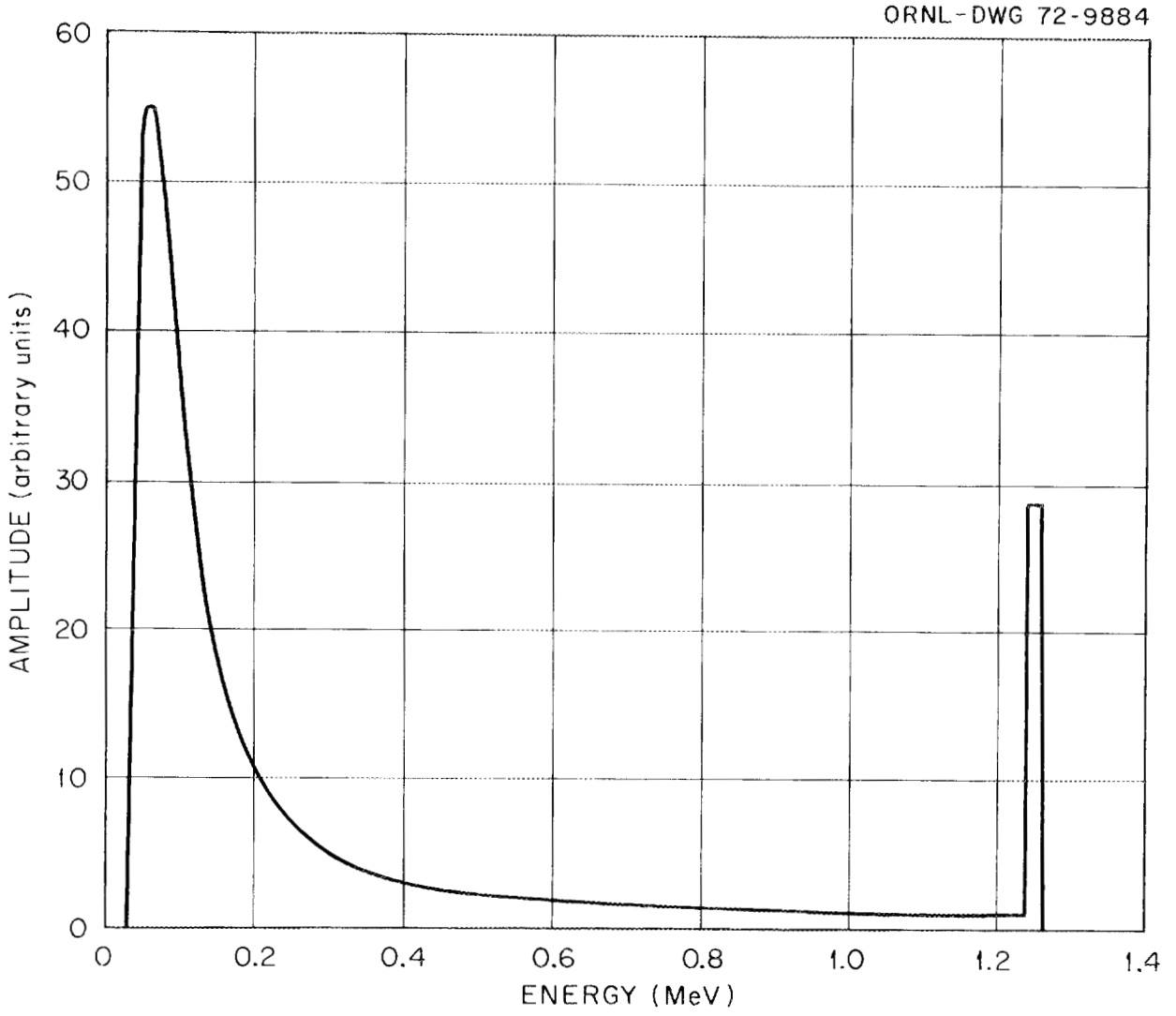

Fig. 10. Calculated gamma-ray energy spectrum at the center of an RSN-81A detector, with water between the detector and ^{60}Co source and a separation distance of 6 in.

A third conclusion is that, if low-energy gamma rays are detected, the response of the detector is drastically increased by the uranium coating on the electrodes, as evidenced by Figs. 7 and 8. Without Pb shielding, the observed increases of I_{DC_γ} are for detectors with electrodes coated with 1 mg/cm^2 of uranium; however, for typical detectors with 2-mg/cm^2 electrode coating, the output would be twice as great.

A general conclusion is that it is essential to avoid detection of low-energy gamma rays for operation of a fission counter in a high gamma background. In any reactor application, an appreciable part of the gamma rays occurring at the location of the fission counter will have a low-energy component because of Compton scattering in the material surrounding the detector; therefore, shielding would be required. A 0.05- to 0.10-in.-thick Pb shield or equivalent would be sufficient for this purpose. An extreme example would be a PCP II-102 fission counter coated with 2 mg/cm^2 of uranium, where a 0.10-in,-thick Pb shield would reduce the I_{DC_γ} by a factor 7.3 and 4.75 for the 15-in. and 6-in. separation distances, respectively, between the ^{60}Co gamma source and the detector in water.

2.3 Selection of a Gamma Shield for Fission Counters

For high-temperature application of fission counters, Pb cannot be used as a gamma shield because of its low melting temperature (327°C, or 621°F); therefore, other high Z materials must be used.

In this selection, the first consideration is the reduction in the neutron detection sensitivity caused by the gamma shielding material. One-dimensional transport calculations using ANISN[3] have been made for tungsten (W), molybdenum (Mo), zirconium (Zr), and lead (Pb) (Fig. 11). Other high-Z materials such as tantalum, platinum, etc., were not considered because of high cost, neutron cross section, or melting point considerations. In Fig. 11, the percentage decrease of neutron detection efficiency is plotted as a function of shield thickness for a fission counter located in the Low-Level Flux Monitor (LLFM) thimble of the Fast Flux Test Facility (FFTF).

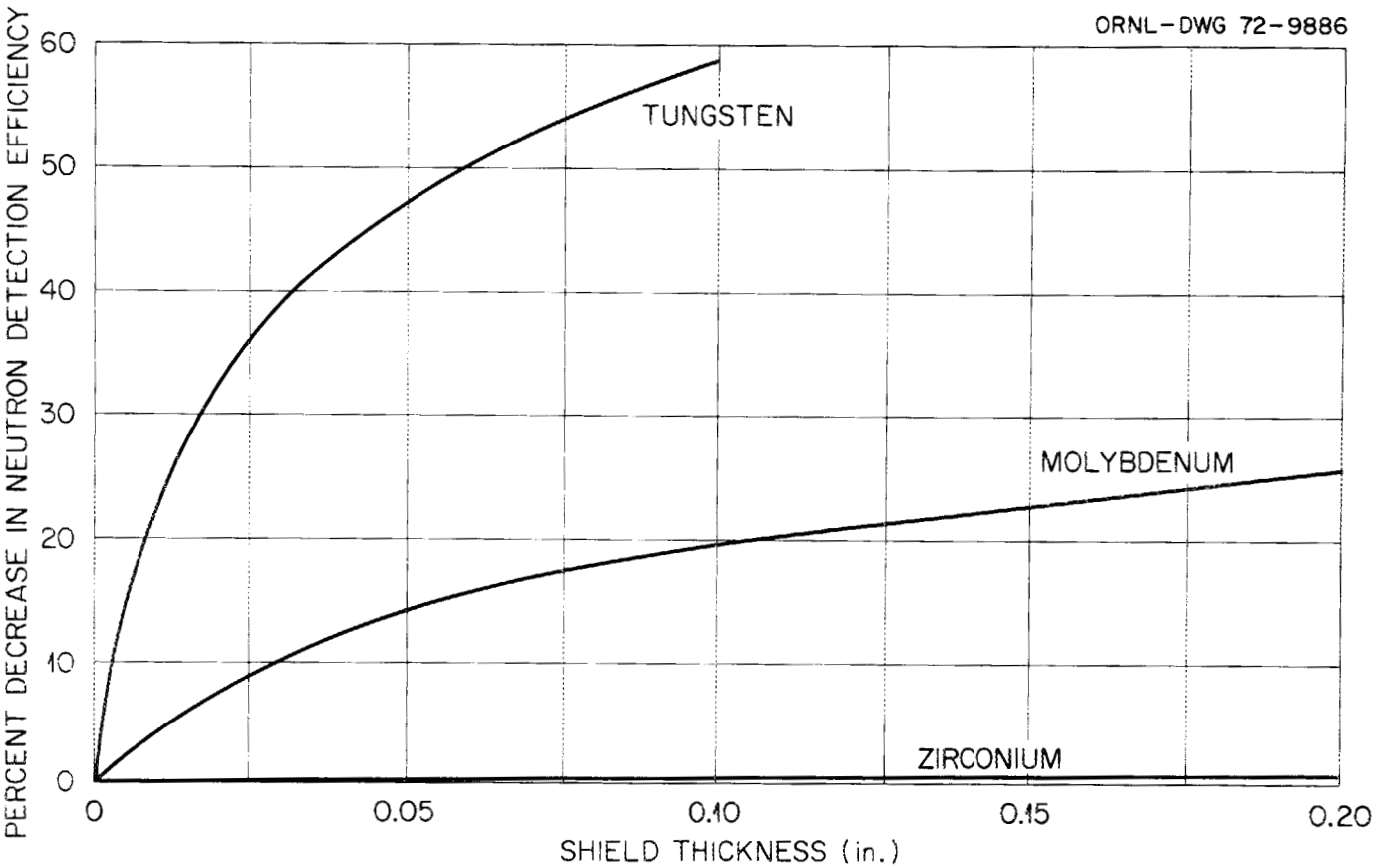

Fig. 11. Effect of shield on neutron detection efficiency of a fission counter located in the Low-Level Flux Monitor of the Fast Flux Test Facility.

From these data it is clear that, if a minimum shield thickness of 0.05 in. must be used, W cannot be used because the possible reduction in GPU would be offset by a loss of neutron sensitivity. The practical choice of shield material is limited to Zr.

The thickness of Zr required to appreciably reduce the GPU effect was determined using the narrow-beam transmission equation:

$$T(E) = e^{-\mu(E)d\rho} \qquad (2)$$

where μ (E) is total mass gamma absorption coefficient in cm^2/g, d is the shield thickness in cm, ρ is the density in g/cm^3, and E is the gamma-ray energy in MeV. The results of material transmission as a function of thickness and energy in Table 2 show that Zr must be six times as thick as Pb to produce the same gamma shielding effectiveness. With a detector having electrodes coated with 2 mg/cm^2 of uranium, separated 6 in. from the ^{60}Co source, and in water, a Zr shield 0.6 cm thick would reduce the I_{DC_γ} a factor of 2.5.

2.4 Electron Drift Velocity

In the overall optimization of a fission counter, the choice of a gas filling that would yield a fast electron collection time and a minimum GPU effect is important. For reasons such as gas stability and temperature and radiation effects, there are only a few gases and gas mixtures that can meet these requirements.

As part of this program electron drift velocity data were compiled and evaluated. When information was not available, the drift velocities were measured. Figures 12 to 19 present compiled and measured electron drift velocities for He, Ar, and Xe gases and Ar - CO_2, Ar - N_2, and He - Xe gas mixtures.

2.5 General Consideration for Optimization of a Fission Counter

There are two major factors to be considered in the optimization of a fission counter:

1. Minimize the GPU amplitude for a given gamma flux:

$$\frac{r_\gamma}{T}^{1/2} \bar{q}_\gamma \ . \qquad (3)$$

Table 2. Gamma transmission through various shield materials as a function of thickness and energy

Shield Material	Transmission for 0.1 cm			Transmission for 0.6 cm		
	0.1 MeV	0.2 MeV	0.5 MeV	0.1 MeV	0.2 MeV	0.5 MeV
Pb	0.002	0.35	0.84	--	--	--
W	0.0003	0.24	0.78	--	--	--
Mo	0.32	0.77	0.91	--	--	--
Zr	--	--	--	0.017	0.39	0.72

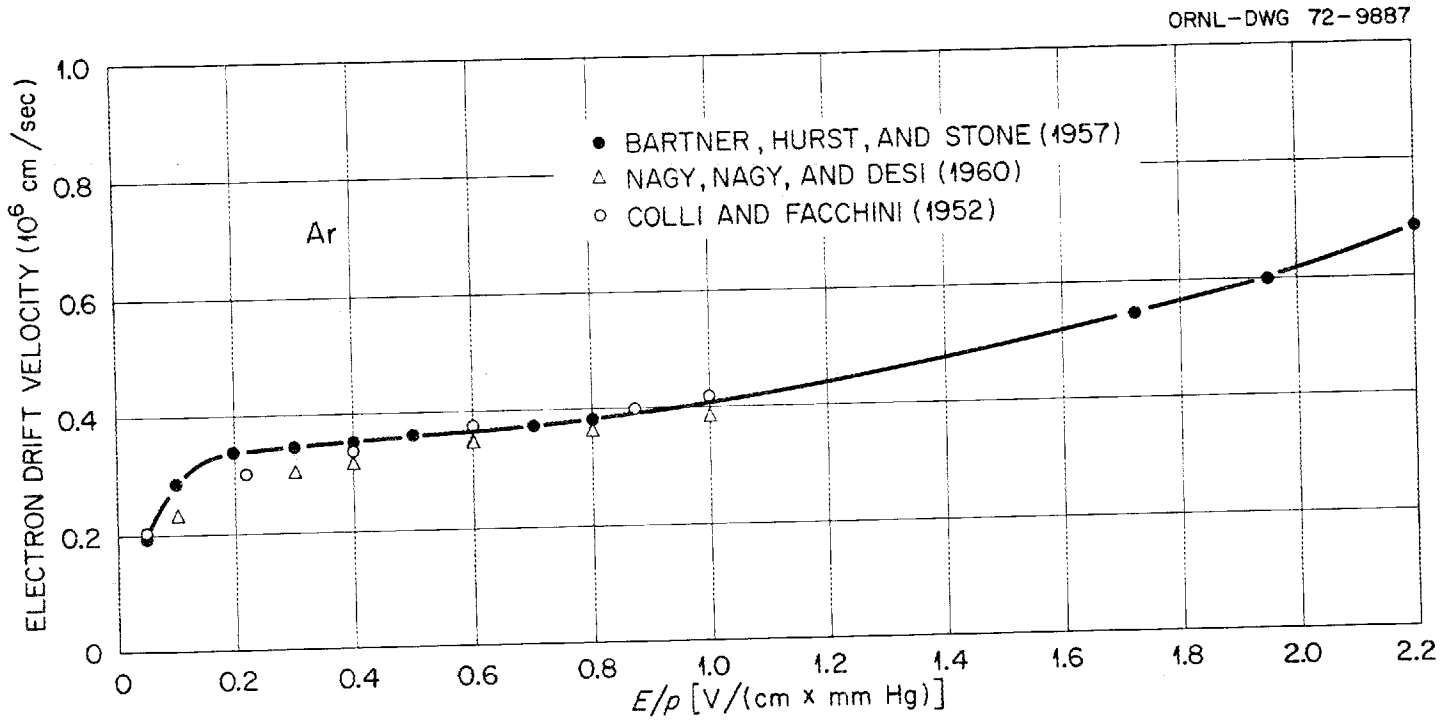

Fig. 12. Electron drift velocity for pure Argon.

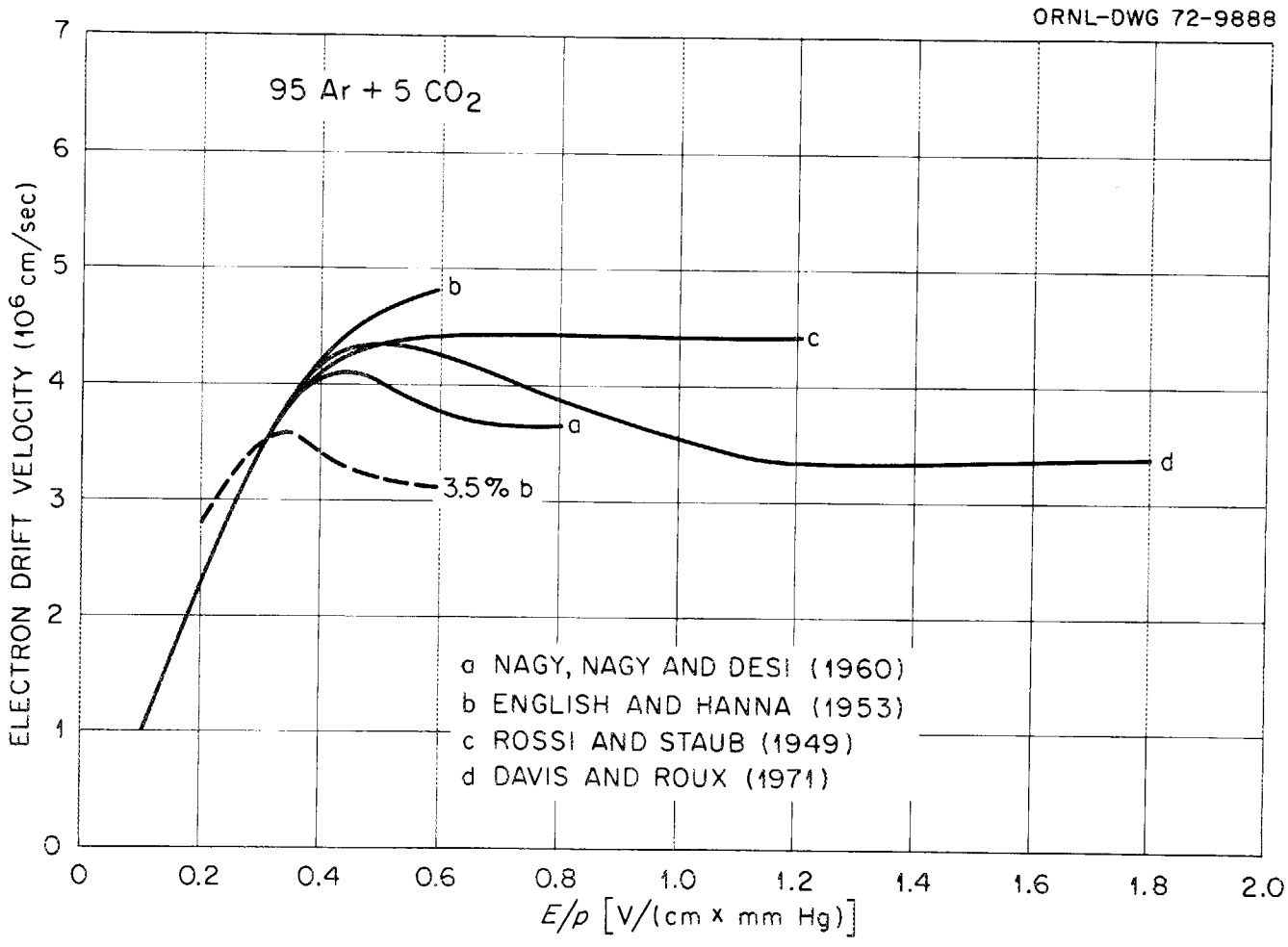

Fig. 13. Electron drift velocities for a gas mixture of 95% Ar and 5% CO_2.

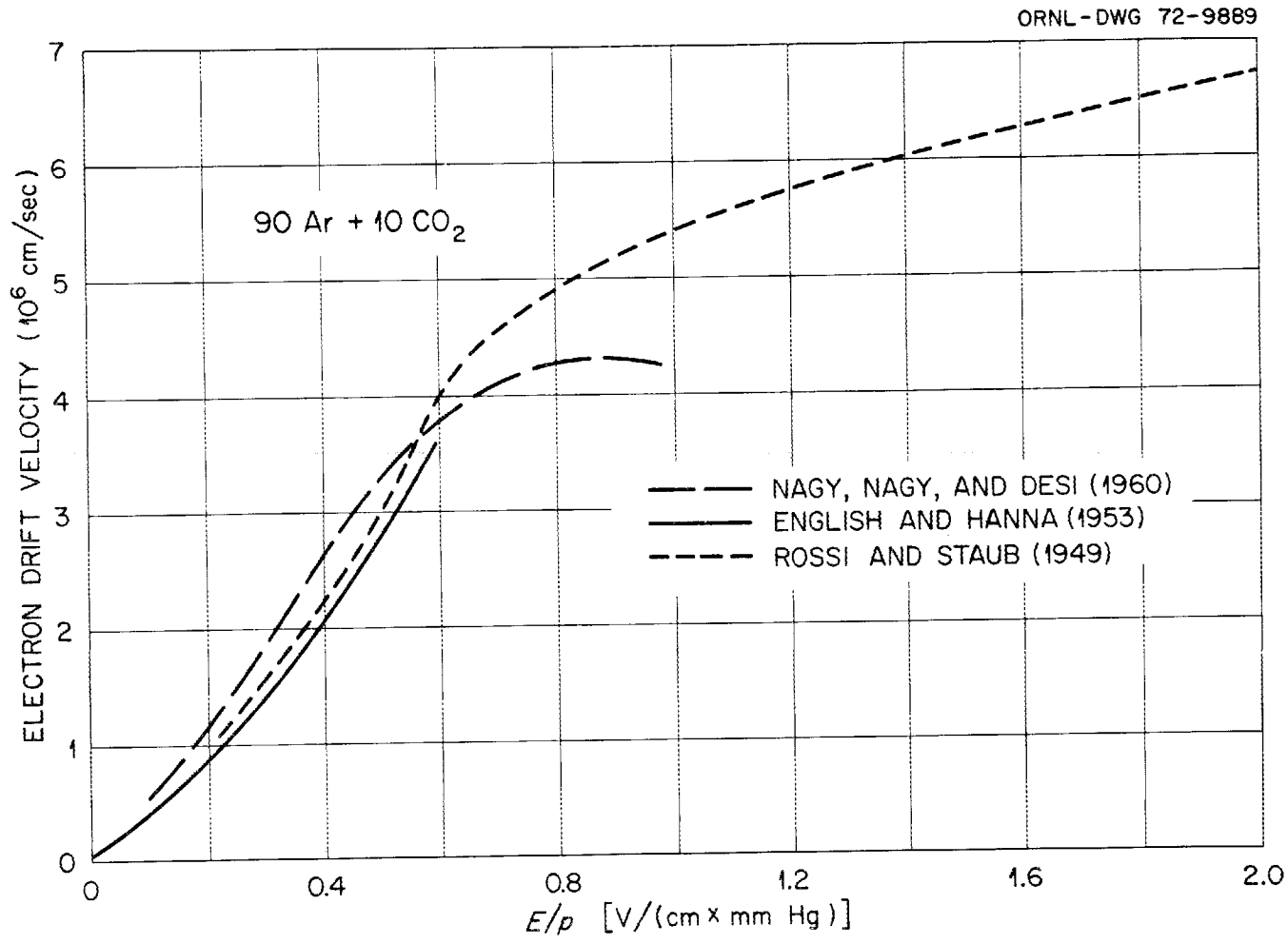

Fig. 14. Electron drift velocities for a gas mixture of 90% Ar and 10% CO_2.

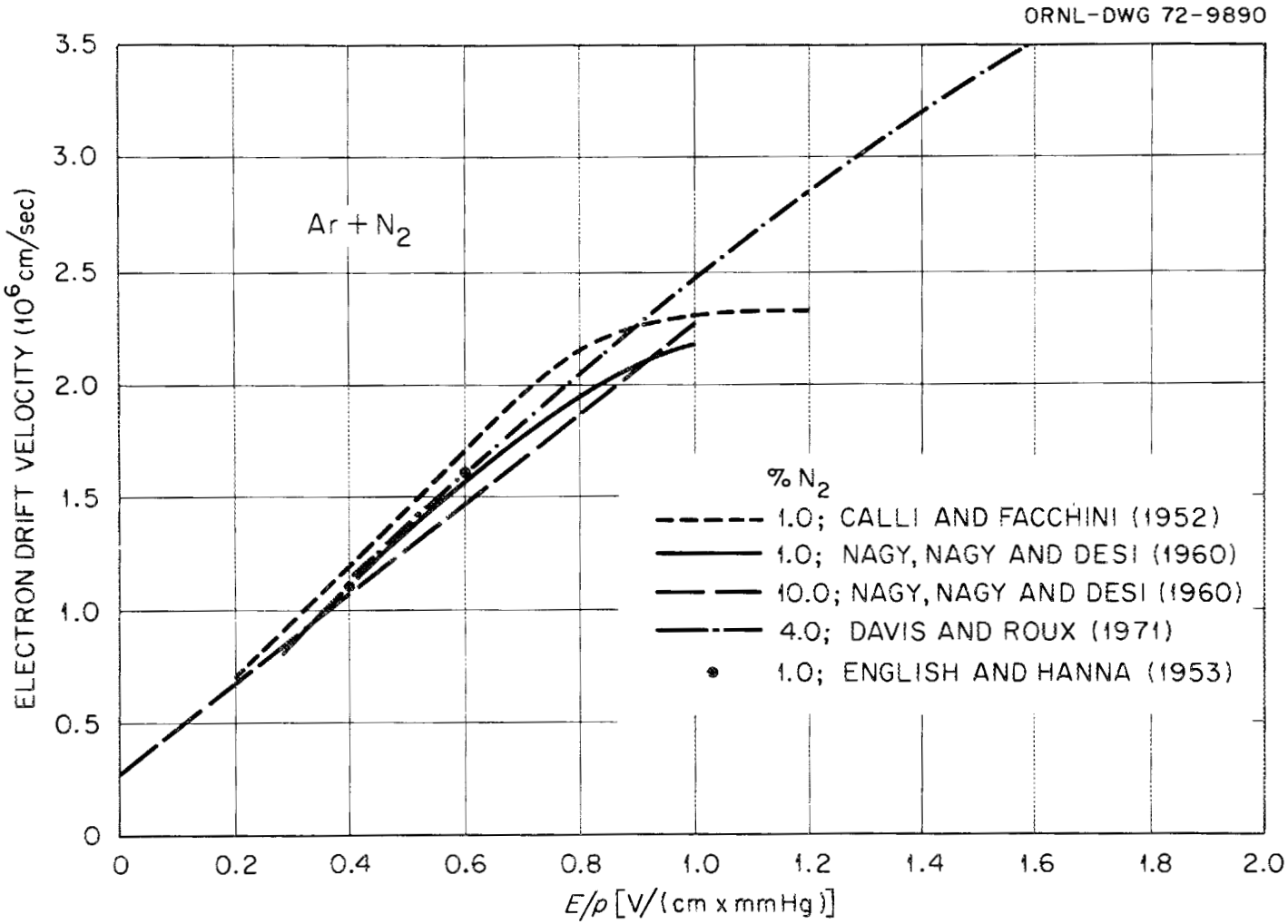

Fig. 15. Electron drift velocities for gas mixtures of Ar and N_2.

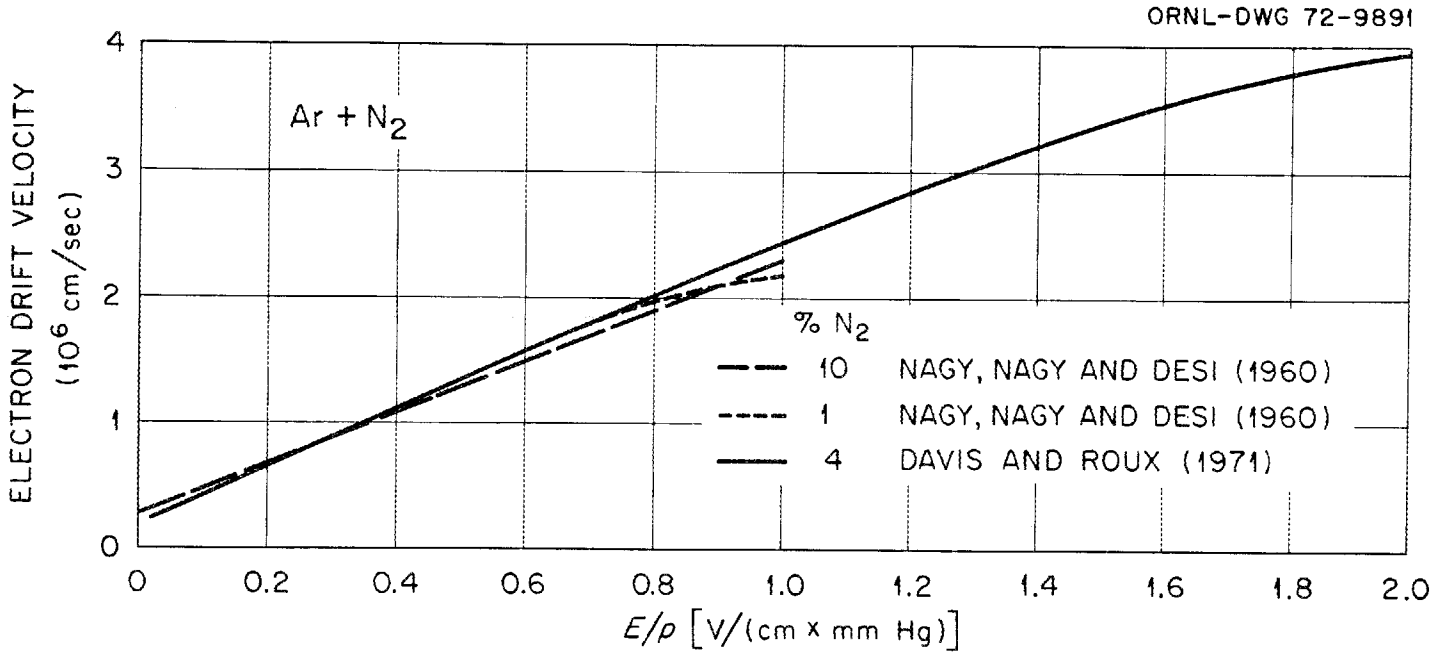

Fig. 16. Electron drift velocities for gas mixtures of Ar and N_2.

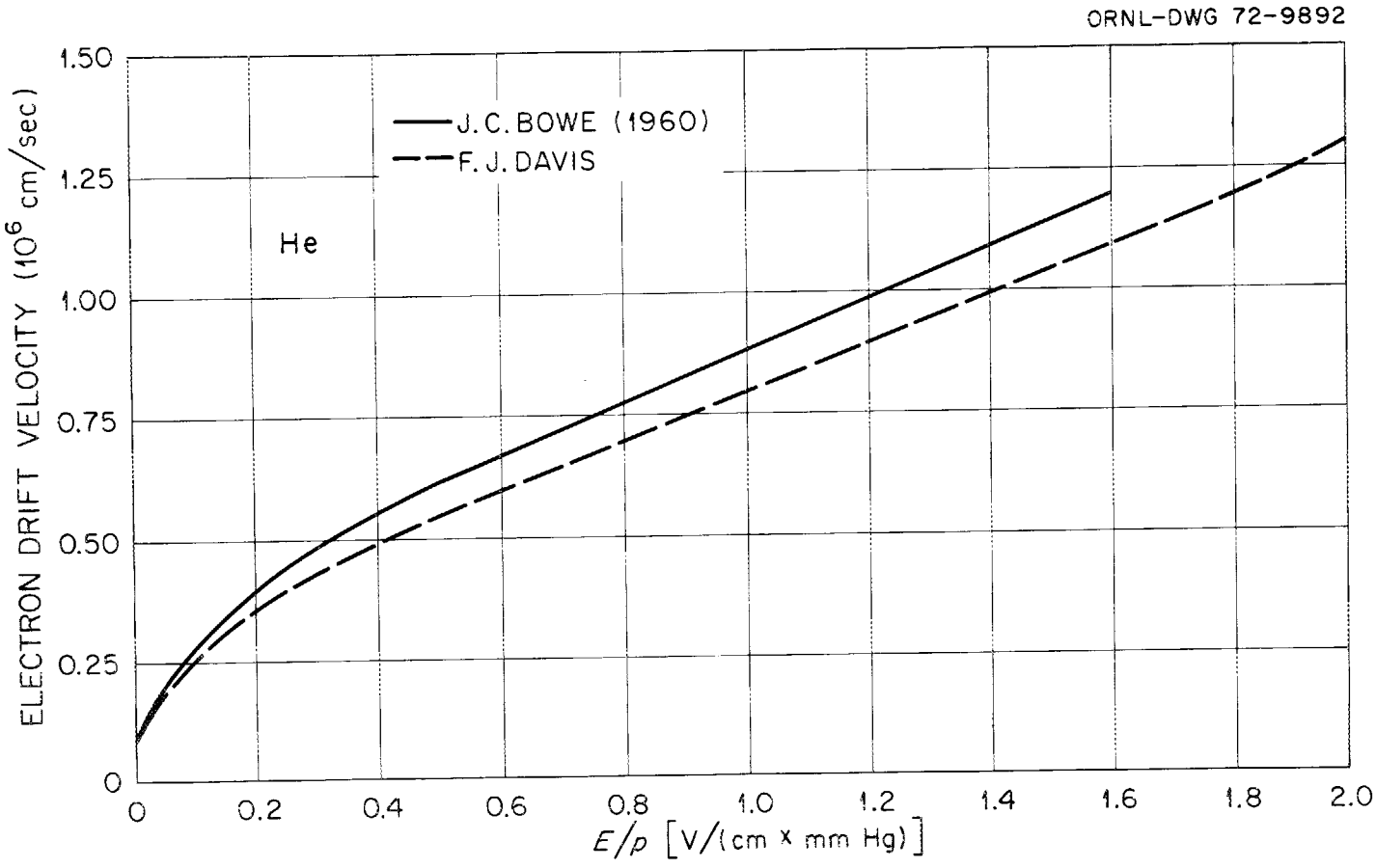

Fig. 17. Electron drift velocity for pure He.

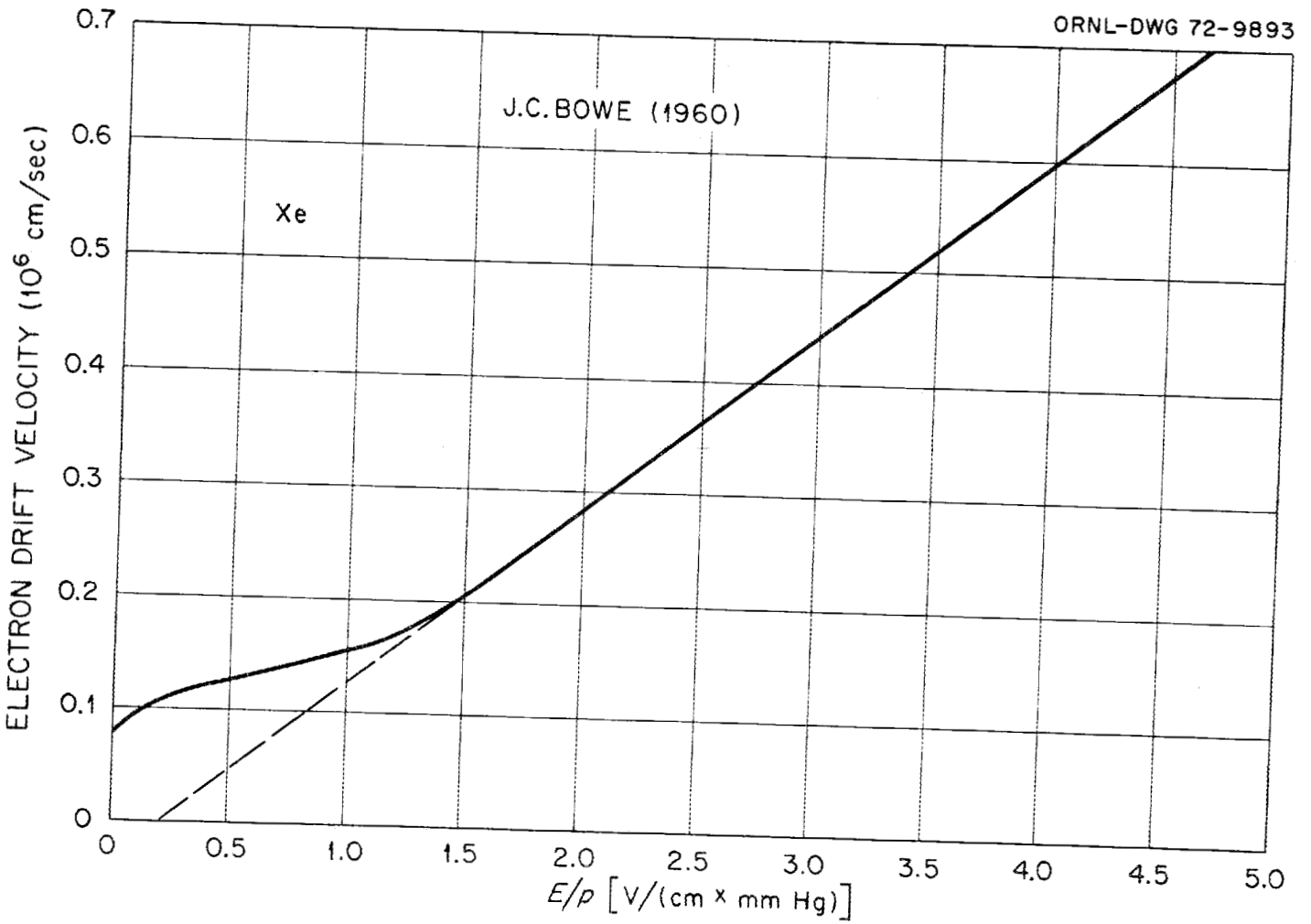

Fig. 18. Electron drift velocity for pure Xe.

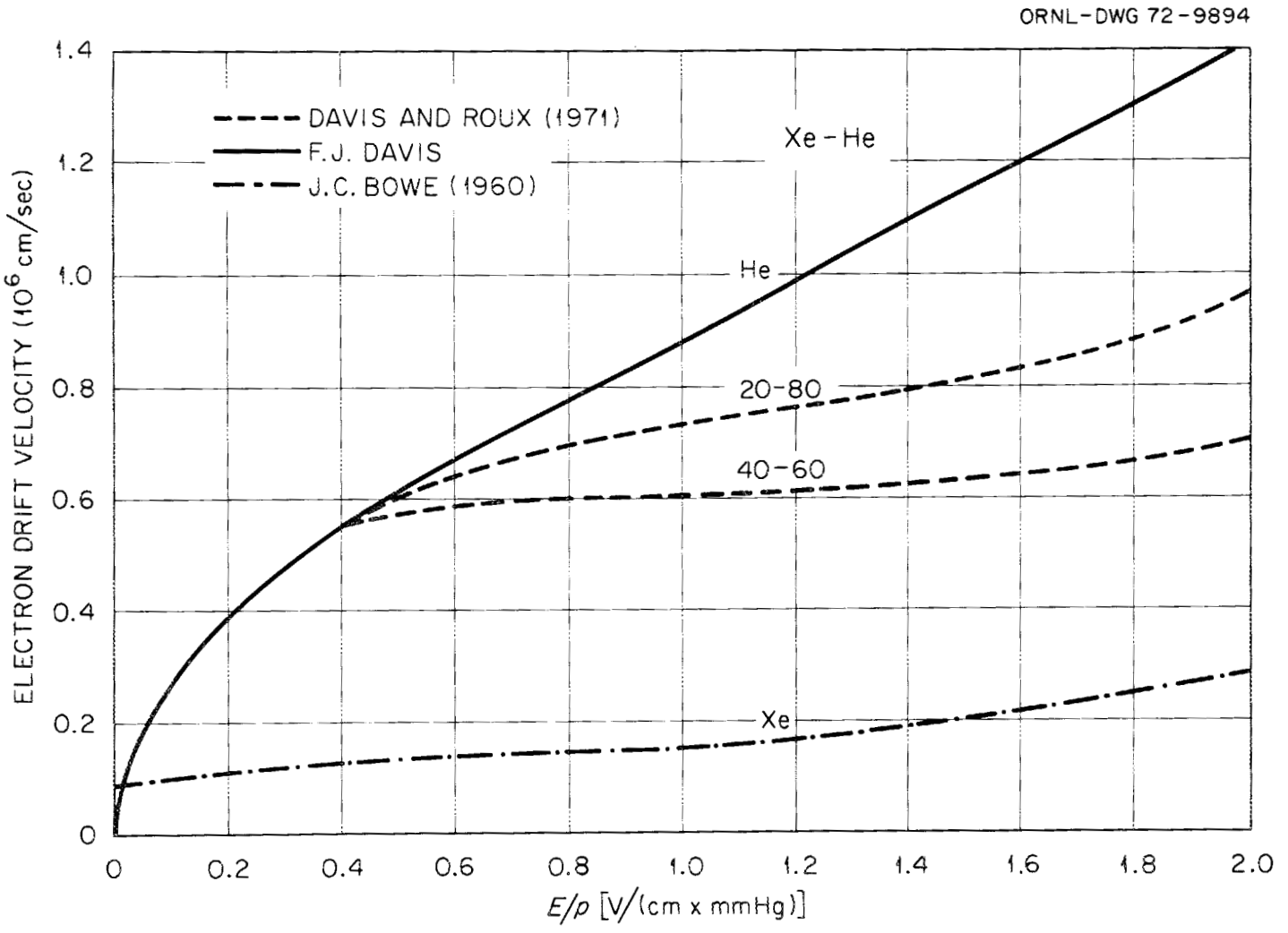

Fig. 19. Electron drift velocities for gas mixtures of He and Xe.

2. Maximize the neutron pulse amplitude:

$$\frac{\overline{q}_n}{\tau} \quad . \tag{4}$$

As a result, the following expression must be maximized:

$$\left(\frac{1}{r_\gamma^{1/2}}\right)\left(\frac{1}{\tau^{1/2}}\right)\left(\frac{\overline{q}_n}{\overline{q}_\gamma}\right), \tag{5}$$

with the constraint that neutron pulses must be much larger than the electronic noise background.

The first consideration is to minimize r_γ which is directly related to the detector gamma sensitivity discussed in Sect. 2.2. It is, therefore, necessary that a gamma shield absorb the low-energy gamma rays. If these low-energy gamma rays are absorbed, S_γ is approximated by

$$S_\gamma = 0.927 \times 10^{-13} \frac{A - hr}{R - cm^3}\left(\frac{Z_{gas}}{Z_{air}} \times \frac{W_{air}}{W_{gas}} \times \frac{p}{760}\right) . \tag{6}$$

The neutron sensitivity consideration governs the required electrode uranium-coating surface area and, therefore, the volume and filling gas pressure p. The electrode spacing d is not a factor in this consideration: if the electrodes are spaced close together, the volume would be reduced but the pressure must be high to absorb the energy of the ionizing fission fragment; conversely, if the electrodes are spaced far apart, the volume would be large but the gas pressure could be made low (because the product of p x d should be maintained constant).

Another optimization consideration is that the electron collection time τ should be as short as possible [Eq. (5)]. To realize this requirement, three actions can be taken:

1. selection of a gas having fast electron-drift velocity characteristics,
2. selection of a close electrode spacing,
3. operation at high E/p values (E is the electrical field between electrodes).

These three choices result from the inspection of the following equation:

$$\tau = \frac{d}{w} , \qquad (7)$$

where w is the electron drift velocity. Operation at high E/p or V/dp is required because, in most cases, the electron drift velocity is a monotonic function of E/p. For the same reason as before, the product of p x d must be maintained constant for a given gas to collect a large share of the energy of the ionizing fission fragments. The highest operating voltage is generally dictated by breakdown pulse noise consideration.

A third optimization consideration is a high $\bar{q}_n/\bar{q}_\gamma$ ratio [Eq. (5)]. In general, this ratio is a weak function of the filling gas. As an example, ratios for different gases were estimated for a p x d product corresponding to the ranges of 25-MeV light fission fragments. The results are presented in Table 3, where the ratios were normalized to 1 for He. In this example (making an abstraction of drift velocity considerations), He has a $\bar{q}_n/\bar{q}_\gamma$ ratio only 40% higher than that for Ar, but the corresponding p x d product is 5.3 times higher. As a result the E/p ratios are 5.3 times lower for a given operating voltage.

In these overall optimization considerations, the discussions of τ and $\bar{q}_n/\bar{q}_\gamma$ ratio were treated separately to provide more insight, but in practice the selections of the fission gas, gas pressure p, and electrode spacing dictate the ratio $\bar{q}_n/\bar{q}_\gamma$, and an overall optimization must be made.

3. ELECTRONICS DEVELOPMENT

Development of a pulse-mode, fast electronics system for optimized operation of a fission counter in a high gamma background has been essentially completed since 1969 and has been reported.[2,4-6] Two areas of new development received attention recently: (1) measurement of electrical shielding effectiveness of high temperature MI coaxial cables, and (2) reduction of electronic noise in current-pulse preamplifiers. Also, RDT Standard C 15-3T, "Current-Pulse Preamplifiers for Use with Fission Counters," was completed, and five units that conform to the standard have been ordered.

Table 3. Comparison of $\bar{q}_n/\bar{q}_\gamma$ ratios for the detection of 25-MeV light fission fragments

Gas or Gas Mixture	p × d Range for 25-MeV Fission Fragments (cm × mm Hg)	Normalized $\bar{q}_n/\bar{q}_\gamma$
He	1368	1.00
N_2	236	1.18
Ar	258	0.71
Xe	137	0.37
Xe–He[a]	486	0.45

[a]0.2 Xe + 0.8 He

3.1 Electrical Shield Performance of High-Temperature MI Coaxial Cables

The electrical shield performance of a 4-mm-OD, SODERN coaxial cable was measured in a range of frequencies from 20 kHz to 10 MHz using a technique previously developed at ORNL[7] (Fig. 20). In the figure calculated data from an equation by Levell[8] are also plotted; the measured and the calculated data are in good agreement. We conclude that the SODERN MI cable incorporated in the design of the fission counter described in Sect. 4 has a shielding effectiveness that is superior to the two-braided RG-223U cable. To demonstrate that Cu is required in the outer sheath of the SODERN cable, calculated data for the same cable but without the Cu are also shown in Fig. 20.

3.2 Reduction of Electronic Noise in Current-Pulse Preamplifier

Two current-pulse preamplifiers (single-ended Q-3125, and differential input Q-5095) were developed for this program. Reduction of the electronic noise was desired for high temperature fission counters, particularly where the neutron plateau characteristics are normally poor.

A slight modification of the input stage, primarily substitution of an MT1061A transistor, reduced the noise threshold for a 10-count/sec background from 15.2 to 11.8 threshold units for the Q-3125 model and from 16.3 to 12.2 for the Q-5095 model. These improvements are for CR-RC main amplifier times-constant values of 27 nsec (refer to Fig. 1).

4. DESIGN AND TEST OF HIGH TEMPERATURE FISSION COUNTER

A fission counter for operation at 750°F has been designed and a prototype is being fabricated. At present, the only acceptable gas mixtures for detector operation at gamma fluxes of 10^6 - 10^7 R/hr are Ar - N_2 mixtures. However, degradation of these gas mixtures occurs at temperatures > 750°F, and thus the temperature limitation is mostly due to the choice of the gas.

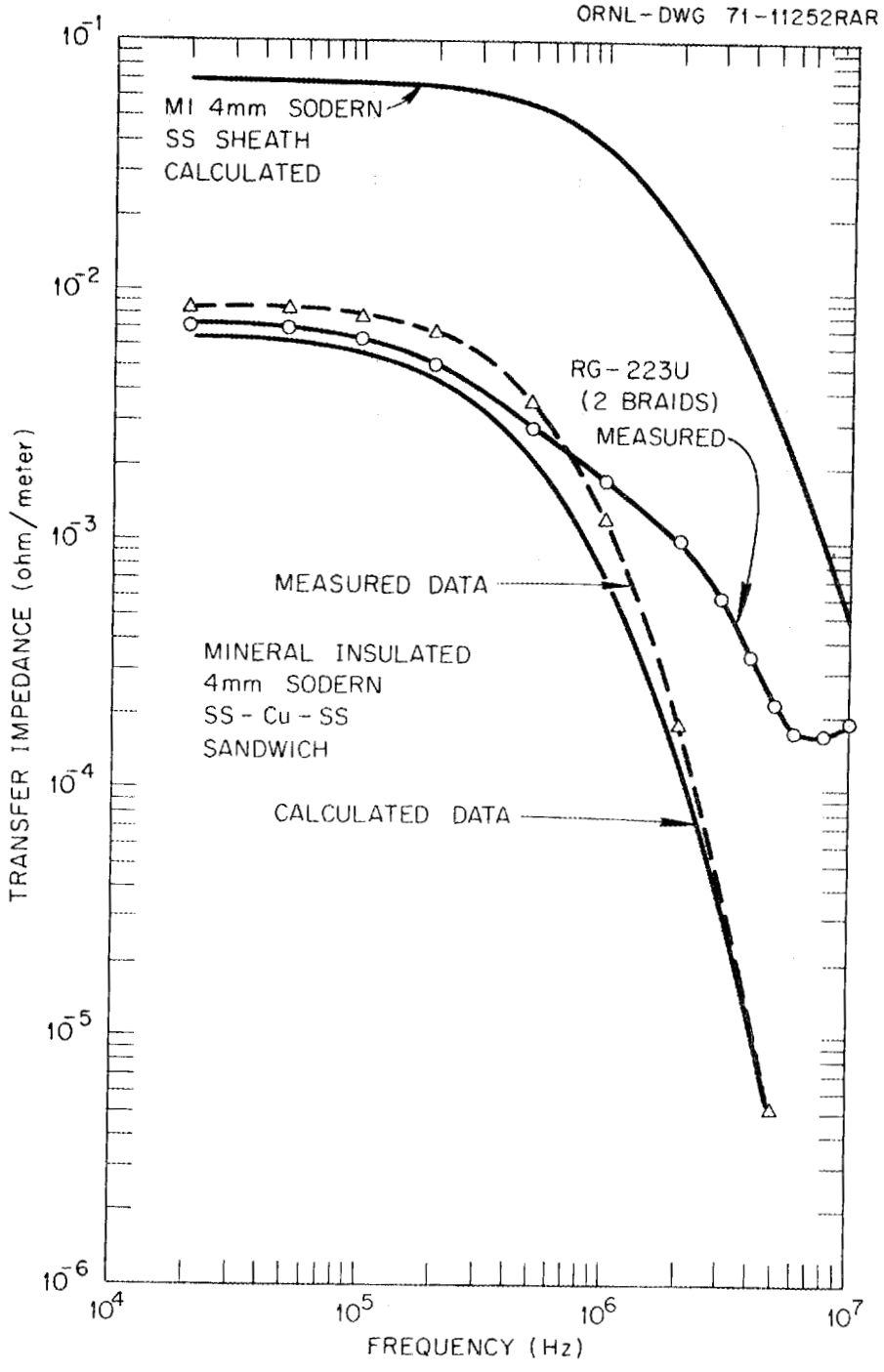

Fig. 20. Coaxial cable electrical shield performance.

Testing of SODERN, mineral-insulated coaxial cable and QUARTEX insulator endseals at 800 V and 1000°F is in progress for qualification at 400 V and 750°F operation.

A program report will be prepared that will describe the detector design and performance after the first series of detailed tests of the prototype are completed.

4.1 Design Characteristics of a 750°F Fission Counter

The design of the fission counter for operation at 750°C is based on the optimization studies reported (Sect. 2). The basic characteristics of the detector are:

Gas pressure:	1900 mm Hg (2.5 atm)
Sensitive area:	1063 cm^2
Electrode spacing:	0.15 cm (0.060 in.)
Sensitive volume:	84.1 cm^3
Gas filling:	0.90 Ar - 0.10 N_2
Operating voltage:	400 V
Collection time:	47 nsec
Electrode coating:	2 mg/cm^2
Coating material:	U_3O_8
^{235}U enrichment:	>99.9%
Total ^{235}U:	1.90 g.

4.2 Mechanical Characteristics

Shielding:	Zr, 0.230 in.
Diameter:	2.5 in., 3.0 in. with shield
Electrode material:	type 304 stainless steel
Overall length:	10.813 in.
Sensitive length:	7.0 in.

This is a concentric cylindrical electrode configuration insulated from the detector shell, with two integral MI cables.

4.3 Sensitivity Data

Neutron (0 R/hr):	1.25 counts/sec $n\bar{v}$ (th)
Neutron (3×10^6 R/hr):	1.0 count/sec $n\bar{v}$ (th)
Neutron (0 R/hr):	2.4×10^{-13} A/$n\bar{v}$ (th)
Gamma:	2.2×10^{-11} A-hr/R with shield
Alpha:	6.0×10^{-10} A.

REFERENCES

1. E. Fairstein and J. Hahn, "Nuclear Pulse Amplifiers--Fundamentals and Design Practice, Part 1," Nucleonics 23(7), 56 (July 1965).

2. D. P. Roux et al., "A Neutron Detection System for Operation in Very High Gamma Fields," Nucl. Appl. and Technol. 9, 736-43 (November 1970).

3. W. W. Engle, A User's Manual for ANISN, A One-Dimensional Discrete Ordinates Transport Code with Anistropic Scattering, K-1693 (March 1967).

4. N. J. Ackermann, Jr., and A. R. Buhl, LMFBR Subcriticality Measurement System Development, ORNL CF-69-11-18 (November 1969).

5. N. J. Ackermann, Jr., and A. R. Buhl, LMFBR Subcriticality Measurement System Development, ORNL CF-70-1-31 (January 1970).

6. N. J. Ackermann, Jr., and A. R. Buhl, LMFBR Subcriticality Measurement System Development, ORNL CF-70-7-52 (July 1970).

7. J. T. De Lorenzo, "Measurement of the Shielding Effectiveness of Coaxial and Two-Conductor Cables," Rev. Sci. Instr. 43(1), 161-164 (January 1972).

8. R. W. Levell, A Preliminary Study of the Characteristics of Mineral Insulated Cables for Reactor Control Pulse Counting Channels, Atomic Energy Establishment, Winfrith, AEEM-369 (Sept. 1963).

ORNL-TM-3959
UC-79m – Liquid Metal Fast
Breeder Reactors
(Instrumentation and Controls)

INTERNAL DISTRIBUTION

1. R. K. Abele, ORNL
2-6. N. J. Ackermann, Jr., ORNL
7. A. R. Buhl, ORNL
8. C. J. Borkowski, ORNL
9-13. W. T. Clay, ORNL
14. F. J. Davis, ORNL
15. J. T. De Lorenzo, ORNL
16. D. N. Fry, ORNL
17. G. C. Guerrant, ORNL
18. W. O. Harms, ORNL
19. W. H. Jordan, ORNL
20. R. C. Kryter, ORNL
21. M. V. Mathis, ORNL
22. L. C. Oakes, ORNL
23. J. C. Robinson, Consultant
24. P. Rubel, ORNL
25. G. S. Sadowski, ORNL
26. D. B. Trauger, ORNL
27-28. Central Research Library
29. Document Reference Section
30-31. Laboratory Records Department
32. Laboratory Records, ORNL R.C.
33. ORNL Patent Office

EXTERNAL DISTRIBUTION

34. Research and Technical Support Division, ORO
35. RDT Senior Site Representative, ORNL
36-37. Director, Div. of Reactor Development and Technology
38-240. Given distribution as shown in TID-4500 under UC-79m – Liquid Metal Fast Breeder Reactors (Instrumentation and Controls) category